Eur. Phys. J. C (2025) 85:39
https://doi.org/10.1140/epjc/s10052-025-13757-2

THE EUROPEAN PHYSICAL JOURNAL C

Regular Article - Theoretical Physics

Thermalization in Krylov basis

Mohsen Alishahiha[1,a], **Mohammad Javad Vasli**[1,2,b]

[1] School of Physics, Institute for Research in Fundamental Sciences (IPM), Tehran 19395-5531, Iran
[2] Department of Physics, University of Guilan, Rasht 41335-1914, Iran

Received: 31 July 2024 / Accepted: 29 December 2024

Abstract We study thermalization in closed non-integrable quantum systems using the Krylov basis. We demonstrate that for thermalization to occur, the matrix representation of typical local operators in the Krylov basis should exhibit a specific tridiagonal form with all other elements in the matrix being exponentially small, reminiscent of the eigenstate thermalization hypothesis. Within this framework, we propose that the nature of thermalization, whether weak or strong, can be examined by the infinite time average of the Krylov complexity. Moreover, we analyze the variance of Lanczos coefficients as another probe for the nature of thermalization. One observes that although the variance of Lanczos coefficients may capture certain features of thermalization, it is not as effective as the infinite time average of complexity.

1 Introduction

Based on our everyday experience, the thermalization of macroscopic systems is one of the most natural phenomena in nature. Although to see a macroscopic system is approaching thermal equilibrium one does not need to produce several copies of the system, the statistical mechanics in which we are dealing with "ensembles" is provided a powerful tool to study thermalization. This has to do with the ergodic property of classical chaotic systems that validates the statistical mechanics. In fact in these systems the ensemble averages used in statistical mechanics calculations agree with the time averages involving in our experiments.

Even though for closed quantum systems one may also observe emerging of the thermal equilibrium in non-equilibrated systems (caused by e.g. global quench), unlike the classical systems, the thermalization may be seen without performing any time averages [1,2]. Indeed, out of equilibrium states approach to their thermal expectations shortly after relaxation. It is, however, important to note that in closed quantum systems dynamics is unitary and time reversal invariant, and therefore, a priori, it is not obvious how and in what sense the thermal equilibrium can be reached dynamically.

The notion of thermalization in quantum mechanics may be described by the eigenstate thermalization hypothesis (ETH) [1,2] which gives an understanding of how an observable thermalizes to its thermal equilibrium value. According to ETH for sufficiently complex quantum systems the energy eigenstates are indistinguishable from thermal states with the same average energy.

Although, it is believed that a non-integrable model will generally thermalize, the nature of thermalization might differ in different situations. Actually, besides Hamiltonian which gives dynamics of the system, the nature of the thermalization may also depend on the initial state, such that, within a fixed model different initial states may exhibit different behaviors [3].

To explore this point better let us consider spin$-\frac{1}{2}$ Ising model given by the following Hamiltonian

$$H = -J \sum_{i=1}^{N-1} \sigma_i^z \sigma_{i+1}^z - \sum_{i=1}^{N} (g\sigma_i^x + h\sigma_i^z)\,. \tag{1}$$

Here and in what follows $\sigma^{z,y,z}$ are Pauli matrices and J, g and h are constants which define the model. By rescaling one may set $J = 1$, and the nature of the model, being chaotic or integrable, is controlled by constants g and h. In particular, for $gh \neq 0$ the model is non-integrable. In what follows to perform our numerical computations we will set $h = 0.5$, $g = -1.05$ [3]. It has been shown in [3] that three different initial states in which all spins are aligned on x, y or z directions denoting by $|X+\rangle, |Y+\rangle, |Z+\rangle$ respectively, results in three distinct thermalization behaviors.

[a] e-mail: alishah@ipm.ir
[b] e-mail: vasli@phd.guilan.ac.ir (corresponding author)

Published online: 21 January 2025

In general, we would like to study time evolution of expectation value of a local operator (observable) $\mathcal{O}$

$$\langle\psi(t)|\mathcal{O}|\psi(t)\rangle = \mathrm{Tr}\left(e^{-iHt}\rho_0 e^{iHt}\mathcal{O}\right), \tag{2}$$

whose behavior could explore the nature of thermalization whether it is strong or weak. In the strong thermalization, the expectation value relaxes to the thermal value very fast, while for weak thermalization it strongly oscillates around the thermal value, though its time average attains the thermal value. Here ρ_0 is density state associated with the initial state $|\psi_0\rangle$.

For the Ising model (1) it has been shown that although the initial state $|Y+\rangle$ exhibits strong thermalization, for initial state $|Z+\rangle$ one observes weak thermalization and for initial state $|X+\rangle$ there is an apparent departure of the thermal expectation value form its thermal value suggesting that there might be no thermalization for this state[1] [3].

It was proposed in [3] that whether we are going to observe strong or weak thermalization is closely related to the effective inverse temperature, β, of the initial state which can be read from the following equation

$$\mathrm{Tr}\,(H(\rho_0 - \rho_{th})) = 0, \tag{3}$$

where $\rho_{th} = \frac{e^{-\beta H}}{\mathrm{Tr}(e^{-\beta H})}$ is thermal density state with inverse temperature β. The strong thermalization occurs when the effective inverse temperature of initial states is close to zero. On the other hand, for initial states whose effective inverse temperature are sufficiently far away from zero, one observes weak thermalization. In particular, for the model given in (1) the initial state $|Y+\rangle$ has zero effective inverse temperature and for initial states $|Z+\rangle$ and $|X+\rangle$ one has $\beta = 0.7275$ and $\beta = -0.7180$, respectively.

For a given initial state $|\psi_0\rangle$ the Eq. (3) may be rewritten as follows

$$\mathrm{Tr}\,(\rho_{th}H)) = \langle\psi_0|H|\psi_0\rangle = E\,, \tag{4}$$

which suggests that the information of the effective inverse temperature could be read from the expectation value of the energy. Indeed, the regime on which the strong or weak thermalization may occur could also be identified by the normalized energy of the initial state [5]

$$\mathcal{E} = \frac{\langle\psi_0|H|\psi_0\rangle - E_{min}}{E_{max} - E_{min}} \tag{5}$$

where E_{max}, E_{min} are maximum and minimum energy eigenvalues of the Hamiltonian. Actually, the quasiparticle explanation of weak thermalization suggests that initial states with weak thermalization are in the regime of near the edge of energy spectrum [6].

Although in the literature, mainly, the normalized energy (5) has been considered to study weak and strong thermalization, it is found useful to work with the expectation value of energy itself which contains the same amount of information as that of the normalized energy.

To further explore the nature of thermalization in the Ising model (1), let us consider an arbitrary initial state in the Bloch sphere which may be parameterized by two angles θ and ϕ as follows[2]

$$|\theta,\phi\rangle = \prod_{i=1}^{N}\left(\cos\frac{\theta}{2}\ |Z+\rangle_i + e^{i\phi}\sin\frac{\theta}{2}\ |Z-\rangle_i\right), \tag{6}$$

where $|Z\pm\rangle$ are eigenvectors of σ^z with eigenvalues $\pm$. Indeed, at each site, the corresponding state is the eigenvector of the operator $\mathcal{O}_i = n\cdot\sigma_i$, with n is the unit vector on the Bloch sphere. More explicitly, one has

$$\mathcal{O}_i(\theta,\phi) = n\cdot\sigma_i = \cos\theta\ \sigma_i^z + \sin\theta\,(\cos\phi\,\sigma_i^x + \sin\phi\ \sigma_i^y), \tag{7}$$

for $i = 1,\ldots,N$.

For this general initial state and for the model (1) one can compute the expectation value of energy which has the following simple form

$$E = -\cos\theta\,(Nh + (N-1)J\cos\theta) - Ng\cos\phi\ \sin\theta\,. \tag{8}$$

An interesting feature of the expectation value of energy is that for large N ($N \gg 1$), the number of spins appears as an overall factor and thus the density of energy defined by E/N (energy per site) is independent of the size of the system

$$\frac{E}{N} \approx -\left(h\cos\theta + J\cos^2\theta\right) - g\cos\phi\ \sin\theta, \quad N \gg 1. \tag{9}$$

Using this analytic expression for the expectation value of energy we have drawn the density of energy in Fig. 1 for $N = 100$ and $J = 1$, $h = 0.5$, $g = -1.05$. Actually, to highlight the regions where the density of energy vanishes we have depicted its absolute value.

To compare this result with the behavior of the effective inverse temperature and in particular the sensitivity of the result with the size of the system, in Fig. 2 we have presented the numerical result of the absolute value of the effective inverse temperature for $N = 7$. Since the Hamiltonian of the

[1] Actually it seems that the apparent departure of thermalization in this case is due to the finite N effects and indeed, even in this case we still have a weak thermalization [4].

[2] In general the initial state could be identified by $2N$ angles (θ_i, ϕ_i) for $i = 1,\ldots N$. In our case we have assumed that angles in all sites are equal.

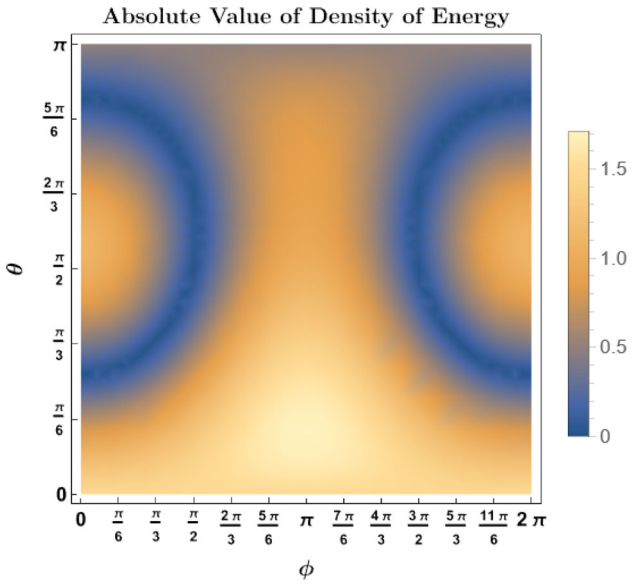

Fig. 1 Absolute value of the density of energy evaluated using the analytic expression (8) for $N = 100$ and $J = 1,\ h = 0.5,\ g = -1.05$

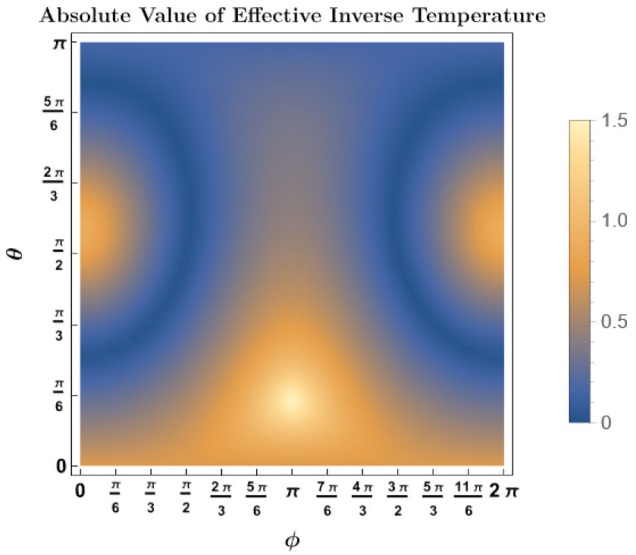

Fig. 2 Absolute value of the effective inverse temperature for arbitrary θ, ϕ for the general initial state (6). Here we have set $N = 7$ and $g = 0.5,\ h = -1.05$

model (1) is traceless, the locus of $\beta = 0$ are given by the regions over which $E = 0$ that are shown by two dark semi circles (ring of zero β[3]) in Figs. 1 and 2. This is, particularly, illustrative since the main significant information contained in β is its distance (absolute value) from zero. Generally, it is believed that strong thermalization occurs near the ring of zero β.

One observes that the behavior of the effective inverse temperature matches exactly that of the density of energy event though the size of the two systems by which these quantities are evaluated are different by about a factor of 15. This shows the robustness of the results against the size of the system. In particular, this has to be compared with the results in the literature where the numerical computations have been performed for $N = 14$. Even though our β is evaluated for $N = 7$ in comparison with that of $N = 14$ the error we acquire is about $\mathcal{O}(1)$ percent.

This article aims to study quantum thermalization using the Krylov basis which seems to be a more appropriate basis when the dynamics of the system is our interest. Although the Krylov method has been used to study numerical computations [7], in recent years there have been several activities to use the Krylov method in the context of quantum chaos (see [8] and its citations).

In this paper, we would like to explore a potential application of Krylov space within the context of quantum thermalization. The key advantage of studying thermalization in this framework lies in the fact that, under a unitary time evolution the trajectory of a given initial state does not necessarily expose into the entire Hilbert space. Instead, it remains confined within a subset known as the Krylov space, which typically has a smaller dimension compared to the full Hilbert space of the system. Thus, focusing on the Krylov space suffices for studying the time evolution of the system. In particular, if the system has conserved charges, working in this basis we are automatically confined in a subsystem that preserves the symmetry of the initial state.

The paper is organized as follows. In the next section, we will study the late time behavior of the expectation value of typical operators within the Krylov basis. Following the Eigenstate Thermalization Hypothesis (ETH), we will propose an ansatz for the matrix elements of the operator within the Krylov basis, called the Krylov Thermalization Hypothesis (KTH). We will present several numerical computations in support of our ansatz. In section three we will study the nature of thermalization in this framework. Specifically, we will introduce two metrics to probe the nature of thermalization-namely, the variance of Lanczos coefficients and the infinite time average of Krylov complexity. While the former may not provide a definitive conclusion, the latter offers a pattern that agrees perfectly with other proposed probes in the existing literature. Additionally, we will calculate the inverse participation ratio to contrast it with the results from the infinite time average of complexity. The late section is devoted to discussions.

[3] By a phase shift one may draw the density of energy for $-\pi \leq \phi \leq \pi$ for which $\beta = 0$ region is a ring.

2 Krylov basis and thermalization

Let us consider a closed quantum system with time independent local Hamiltonian H whose eigenstates and eigenvalues are denoted by $|E_n\rangle$, and E_n, respectively. Starting with an initial state, $|\psi_0\rangle$, in the Schrödinger picture at any time one has

$$|\psi(t)\rangle = e^{iHt}|\psi_0\rangle\,. \tag{10}$$

In the context of quantum thermalization the main purpose is to start with an initial state and then quickly alter the system, e.g. by a global quench, and then let the system evolve under the local Hamiltonian H. As we have already mentioned, generally, we are interested in the late time behavior of the expectation value of local operators (observables)

$$\langle\psi(t)|\mathcal{O}|\psi(t)\rangle = \langle\psi_0|e^{-iHt}\mathcal{O}e^{iHt}|\psi_0\rangle = \langle\mathcal{O}(t)\rangle\,. \tag{11}$$

The main question is to what extent and for what times the system can be described by a suitable thermal equilibrium system in which the above expectation value can be approximated by Tr $(\rho_{th}\mathcal{O})$.

To study different features of chaotic systems and thermalization one usually utilizes the energy spectrum and energy eigenstates which amounts to diagonalize the Hamiltonian. For example, the nature of quantum chaos may be given in terms of the energy level statistics [9].

In the energy eigenstates, assuming $|\psi_0\rangle = \sum_\alpha c_\alpha|E_\alpha\rangle$, the expectation value (11) reads

$$\langle\mathcal{O}(t)\rangle = \mathrm{Tr}(\rho_{DE}\mathcal{O}) + \sum_{\alpha\neq\beta}^{\mathcal{D}} e^{i(E_\alpha-E_\beta)t}c_\alpha c_\beta^*\langle E_\alpha|\mathcal{O}|E_\beta\rangle\,, \tag{12}$$

where ρ_{DE} is diagonal density matrix

$$\rho_{DE} = \sum_{\alpha=1}^{\mathcal{D}}|c_\alpha|^2|E_\alpha\rangle\langle E_\alpha|\,. \tag{13}$$

Here $\mathcal{D}$ is the dimension of Hilbert space. Then, one can proceed to explore equilibrium and thermalization in this context which happens due to the possible phase cancellation at long times [10] when the expectation value of the operator may be given by the canonical ensemble $\mathrm{Tr}(\rho_{DE}\mathcal{O}) \approx \mathrm{Tr}(\rho_{th}\mathcal{O})$.

We note, however, that a Hamiltonian may be also put into a tridiagonal form in which we could work in the Krylov basis. See e.g [11–13]. In this basis, we usually deal with Lanczos coefficients and thus we would expect that the properties of the quantum system can be also described in terms of the spectrum of Lanczos coefficients. Indeed, the Lanczos spectrum has been used to study operator growth in many body systems [8] (see also [14]). Recently, it was also suggested in [13] that the chaotic nature of a system may be described in terms of the Lanczos coefficients. More precisely, it was proposed that "Quantum chaotic systems display a Lanczos spectrum well described by random matrix model."

Here we would like to study quantum thermalization in the Krylov basis. In particular, we would like to understand to what extent the nature of thermalization may be explored in this context (see also [15]). To proceed, let us first briefly review the recursive procedure producing the Krylov space for a given state in a quantum system (see [7] for review).

Starting with an initial state $|\psi_0\rangle$ in a quantum system with a time independent Hamiltonian H, the Krylov basis, $\{|n\rangle, n = 0, 1, 2, \ldots, \mathcal{D}_\psi - 1\}$, can be constructed as follows. The first element of the basis is identified with the initial state $|0\rangle = |\psi_0\rangle$ (which we assume to be normalized) and then the other elements are constructed, recursively, as follows

$$\widehat{|n+1\rangle} = (H - a_n)|n\rangle - b_n|n-1\rangle\,, \tag{14}$$

where $|n\rangle = b_n^{-1}|\hat{n}\rangle$, and

$$a_n = \langle n|H|n\rangle, \quad b_n = \sqrt{\langle\hat{n}|\hat{n}\rangle}\,. \tag{15}$$

This recursive procedure stops whenever b_n vanishes which occurs for $n = \mathcal{D}_\psi \leq \mathcal{D}$ that is the dimension of Krylov space. Note that this procedure produces an orthonormal and ordered basis together with coefficients a_n and b_n known as Lanczos coefficients [16].

Having constructed the Krylov basis, at any time the evolved state may be expanded in this basis

$$|\psi(t)\rangle = \sum_{n=0}^{\mathcal{D}_\psi-1}\phi_n(t)\,|n\rangle\,, \quad \text{with} \quad \sum_{n=0}^{\mathcal{D}_\psi-1}|\phi_n(t)|^2 = 1\,, \tag{16}$$

where the wave function $\phi_n(t)$ satisfies the following Schrödinger equation

$$-i\,\partial_t\phi_n(t) = a_n\phi_n(t) + b_n\phi_{n-1}(t) + b_{n+1}\phi_{n+1}(t)\,, \tag{17}$$

which should be solved with the initial condition $\phi_n(0) = \delta_{n0}$.

Using the completeness of the energy eigenstates one may expand any element of the Krylov basis in terms of energy basis

$$|n\rangle = \sum_{\alpha=1}^{\mathcal{D}} f_{n\alpha}|E_\alpha\rangle\,. \tag{18}$$

Note that since $\mathcal{D}_\psi \leq \mathcal{D}$, the expansion coefficient, $f_{n\alpha}$, is not necessary inevitable and therefore, in general, energy eigenstates cannot be expanded in terms of Krylov basis. Using the orthogonality condition of the Krylov basis one gets

$$\sum_{\alpha=1}^{\mathcal{D}} f^*_{n\alpha} f_{m\alpha} = \delta_{nm} \,. \tag{19}$$

On the other hand from the Eq. (14) one finds

$$f_{n\alpha} E_\alpha = a_n f_{n\alpha} + b_{n+1} f_{n+1\alpha} + b_n f_{n-1\alpha} \,, \tag{20}$$

that can be used to find $f_{n\alpha}$ in terms of $f_{0\alpha} = c_\alpha$.

In this formalism the expectation value of a local operator (11) reads

$$\langle \mathcal{O}(t) \rangle = \sum_{n,m=0}^{\mathcal{D}_\psi - 1} \phi^*_n(t) \phi_m(t)\, O_{nm} \tag{21}$$

where $O_{nm} = \langle n|\mathcal{O}|m\rangle$ are matrix elements of the operator $\mathcal{O}$ in the Krylov basis which, in general, are complex numbers. Of course, the diagonal elements are real.

To find the infinite time average of the corresponding operator one needs to compute C_{nm} given by

$$C_{nm} = \lim_{T\to\infty} \frac{1}{T} \int_0^T dt\, \phi^*_n(t) \phi_m(t) \,, \tag{22}$$

that is essentially matrix elements of the diagonal density matrix in the Krylov basis $C_{nm} = \langle m|\rho_{DE}|n\rangle$, that is

$$C_{nm} = \sum_{\alpha=1}^{\mathcal{D}} |c_\alpha|^2 f_{m\alpha} f^*_{n\alpha} \,. \tag{23}$$

In this framework, inspired by ETH, we propose an ansatz for the matrix elements of typical operators in the Krylov basis to ensure that thermalization occurs within the system. To illustrate how the corresponding ansatz might be formulated, let us consider the ETH ansatz for the matrix elements of the operator $\mathcal{O}$ in energy eigenstates [1,10],[4]

$$\langle E_\alpha|\mathcal{O}|E_\beta\rangle = f(E_\alpha)\delta_{\alpha\beta} + e^{-\frac{S(\bar{E})}{2}} f_{\mathcal{O}}(\bar{E},\omega) R_{\alpha\beta} \,, \tag{24}$$

where $\bar{E} = (E_\alpha + E_\beta)/2$, $\omega = E_\alpha - E_\beta$. This expression can be utilized to propose an ansatz for the matrix elements of the operator $\mathcal{O}$ in the Krylov basis through the following relation

$$\langle n|\mathcal{O}|m\rangle = \sum_{\alpha,\beta=1}^{\mathcal{D}} f^*_{n\alpha} f_{m\beta}\ \langle E_\alpha|\mathcal{O}|E_\beta\rangle. \tag{25}$$

To proceed, one can promote the function f to an operator by replacing the energy with the Hamiltonian

$$f(E_\alpha) \to \hat{f}(H) \,. \tag{26}$$

This allows to express the ETH ansatz as follows

$$\langle E_\alpha|\mathcal{O}|E_\beta\rangle = \langle E_\alpha|\hat{f}(H)|E_\beta\rangle + \mathcal{O}(e^{-S/2}) \,. \tag{27}$$

Here we have utilized the fact that $\hat{f}(H)|E_\beta\rangle = f(E_\beta)|E_\beta\rangle$. Plugging this expression into Eq. (25) one gets

$$\langle n|\mathcal{O}|m\rangle = \langle n|\hat{f}(H)|m\rangle + \text{suppressed terms} \,. \tag{28}$$

In this equation, the suppressed terms correspond to the exponentially suppressed terms in the original ETH ansatz. Using the fact that $\langle n|m\rangle = \delta_{nm}$ and

$$\langle n|H|m\rangle = a_n \delta_{n\,m} + b_{m+1}\delta_{n\,m+1} + b_m \delta_{n\,m-1}, \tag{29}$$

it becomes clear that the matrix representation of the operator $\mathcal{O}$ in the Krylov basis is not diagonal. However, we note that while off-diagonal elements also appear in leading order in this expression, we generally would not expect significant contributions from all off-diagonal matrix elements.

To understand this, we recognize that for thermalization to occur beside the ETH ansatz, one must further assume that f is a smooth and slowly varying function of E_α. Additionally, the initial state must be sufficiently localized within a narrow energy window-specifically, the variance of energy should be much smaller than the energy expectation value of the initial state. This justifies the neglecting of higher-order terms in the following Taylor expansion [10][5]

$$f(E_\alpha) \approx f(E) + (E_\alpha - E)\, f'(E), \tag{30}$$

where $E = \langle\psi_0|H|\psi_0\rangle$ and, $f(E)$ is the expectation value predicted by the (micro)canonical ensemble $\text{Tr}(\rho_{th}\mathcal{O}) \approx f(E)$. Here "prime" denotes derivative with respect to E_α. In this approximation, the ETH ansatz (24) reads

$$\mathcal{O}_{\alpha\beta} \approx f(E)\delta_{\alpha\beta} + f'(E)\,\langle E_\alpha|H - E|E_\beta\rangle + \mathcal{O}(e^{-\frac{S}{2}}) \,, \tag{31}$$

[4] In this expression $S(\bar{E})$ is thermal entropy at energy $\bar{E}$ which is an extensive quantity and proportional to the size of the system. It is important to note that f and f_O are smooth functions of their arguments. $R_{\alpha\beta}$ is a random real or complex variable with zero mean $\overline{R_{\alpha\beta}} = 0$ and unit variance: $\overline{R^2_{\alpha\beta}} = 1$, $\overline{|R_{\alpha\beta}|^2} = 1$.

[5] More precisely, one assumes that $(\Delta E)^2 f''(E)/f(E) \ll 1$ with ΔE being the variance of energy [10].

resulting in the following expression for the matrix elements in the Krylov basis

$$\mathcal{O}_{nm} \approx f(a_0)\delta_{nm} + f'(a_0)\,\langle n|H - a_0|m\rangle \\ +\text{suppressed terms}, \tag{32}$$

which shows that the matrix representation of a typical observable in the Krylov basis is essentially tridiagonal in which the off-diagonal elements adjacent to the diagonal, denoted as $\mathcal{O}_{nn+1}$, are proportional to the Lanczos coefficients b_n (see Eq. (29)). Note that the suppressed terms, which contain b_n-dependent factors, are of order $\mathcal{O}(\Delta E^2)$.

Regarding "suppressed terms," one can follow a similar approach as with the ETH ansatz to estimate their order of magnitude [17]. To proceed, following [18], we note that using the completeness of the Krylov basis, the inequality the fact $\langle n|\mathcal{O}^2|n\rangle \leq |\mathcal{O}|^2$ maybe written as $\sum_m |\mathcal{O}_{nm}|^2 \leq |\mathcal{O}|^2$. Moreover, since $|\mathcal{O}_{nn}|^2$ is always positive one may write

$$\sum_{m(\neq n)=0}^{\mathcal{D}_\psi - 1} |\mathcal{O}_{nm}|^2 \leq |\mathcal{O}|^2 \,. \tag{33}$$

where $|\mathcal{O}|$ denotes the operator norm,[6] and $\mathcal{D}_\psi$ is the dimension of the Krylov space associated with the initial state ψ_0. Moreover, if we assume that the off-diagonal matrix elements $\mathcal{O}_{nm}$ are smooth and vary slowly, they can be considered to be almost constant so that one finds

$$\sum_{m(\neq n)=0}^{\mathcal{D}_\psi - 1} |O_{nm}|^2 \approx |O_{nm}|^2 \sum_{m(\neq n)=0}^{\mathcal{D}_\psi - 1} = |O_{nm}|^2 \mathcal{D}_\psi \,. \tag{34}$$

By making use of this approximation one can derive an expression that captures the behavior of off-diagonal elements to the leading order. Indeed from Eq. (33), we one gets

$$|\mathcal{O}_{nm}| \leq \frac{|\mathcal{O}|}{\sqrt{\mathcal{D}_\psi}} \,. \tag{35}$$

It is essential to highlight that the aforementioned condition pertains to the contributions of "suppressed terms" to off-diagonal matrix elements. Additionally, there is a contribution to these off-diagonal matrix elements from leading terms, as indicated in Eq. (32).

Inspired by the above observations one can propose an ansatz for the matrix elements of typical operators in the Krylov basis as follows

$$\langle n|\mathcal{O}|m\rangle = \langle n|\hat{f}(H)|m\rangle + \frac{1}{\sqrt{\mathcal{D}_\psi}} f_{\mathcal{O}}(a_{nm}) R_{nm} \,, \tag{36}$$

where $a_{nm} = \langle n|H|m\rangle$. Here R_{nm} is a random real or complex variable with zero mean $\overline{R_{nm}} = 0$ and unit variance: $\overline{R_{nm}^2} = 1$, $\overline{|R_{nm}|^2} = 1$.

The Eq. (36) imposes a condition on the matrix elements of the operator $\mathcal{O}$ in the Krylov basis, which can be seen as an ansatz for these matrix elements to ensure thermalization. This is referred to as the KTH ansatz. It is worth noting that, in practice, for typical chaotic systems, the leading-order terms of the KTH ansatz are actually represented by those in Eq. (32). In fact by substituting this expression into Eq. (21) one finds

$$\langle \mathcal{O}(t)\rangle = \sum_{n,m=0}^{\mathcal{D}_\psi - 1} \phi_n^*(t)\phi_m(t)\,\langle n|\hat{f}(H)|m\rangle \\ + \frac{1}{\sqrt{\mathcal{D}_\psi}} \sum_{n,m=0}^{\mathcal{D}_\psi - 1} \phi_n^*(t)\phi_m(t)\, f_{\mathcal{O}}(a_{nm}) R_{nm}. \tag{37}$$

Note that this equation indicates that the off-diagonal terms, which contain b_n-dependent terms, remain exponentially suppressed, scaling as $\mathcal{O}(e^{-S/2})$.

One can use (32) to simplify the first line of the above equation. It is clear that the contribution of off-diagonal term in (32) vanishes,[7] whereas from the first term and taking into account that $\sum_n |\phi(t)|^2 = 1$ one arrives at

$$\langle \mathcal{O}(t)\rangle \approx f(a_0) + \frac{1}{\sqrt{\mathcal{D}_\psi}} \sum_{n,m=0}^{\mathcal{D}_\psi - 1} \phi_n^*(t)\phi_m(t)\, f_{\mathcal{O}}(a_{nm}) R_{nm}, \tag{38}$$

which results in

$$\langle \mathcal{O}(t)\rangle \approx \mathrm{Tr}(\rho_{th}\mathcal{O}) + \text{small fluctuations}, \tag{39}$$

as expected. Here we have used that the system thermalizes so that the expectation value of the operator is equal to thermal expectation value $f(a_0) = \mathrm{Tr}(\rho_{th}\mathcal{O})$. Therefore, even though the matrix is tridiagonal, the main contribution is primarily determined by the diagonal elements, which represent the expectation value of the corresponding operator as derived from the (micro)canonical ensemble. It is also worth noting that in our context, all physical results are fundamentally determined by two parameters: a_0 and b_1, both of which carry physical significance. Specifically, $a_0 = E$ represents the energy of the initial state, while $b_1 = \Delta E$ denotes its variance..

To examine the KTH behavior of local operators (observables) we will compute matrix elements of the operator $S_x = \sum_{i=1}^N \sigma_i^x$, which is magnetization in the x direction,

[6] The norm is defined by $|\mathcal{O}| = \sup_\psi \sqrt{\langle\psi|\mathcal{O}^\dagger\mathcal{O}|\psi\rangle}$ [18].

[7] Note that $\sum_{n,m=0}^{\mathcal{D}_\psi - 1} \phi_n^*(t)\phi_m(t)\,\langle n|H|m\rangle = E$ and by definition $a_0 = E$.

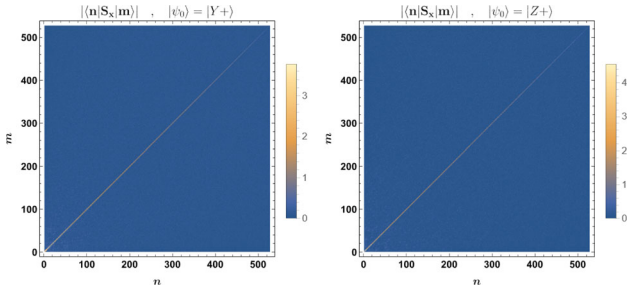

Fig. 3 Matrix elements of the operator $S_x = \sum_i \sigma_i^x$ in Krylov basis for cases where the initial state is $|Y+\rangle$ (left) and $|Z+\rangle$ (right). Darker points represent the matrix elements that are closed to zero. Although, due to its resolution, it might not be clear for these plots, these matrices are not diagonal and, indeed, they are tridiagonal (see Fig. 4)

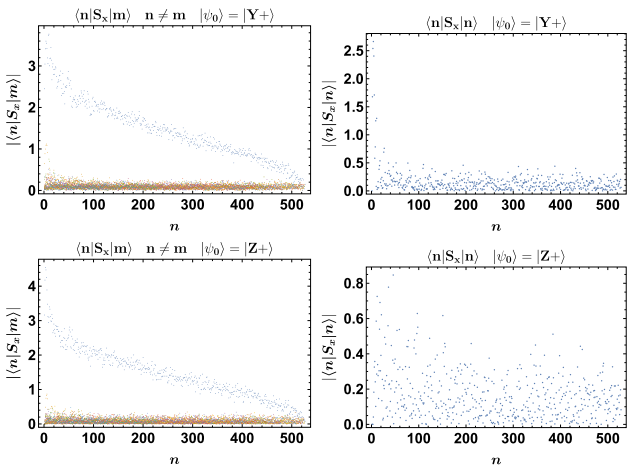

Fig. 4 Actual (absolute) values of matrix elements of the operator $S_x = \sum_i \sigma_i^x$ in Krylov basis for cases where the initial state is $|Y+\rangle$ (up) and $|Z+\rangle$ (down). Blue points in left panels denote $(S_x)_{n,n+1}$ elements

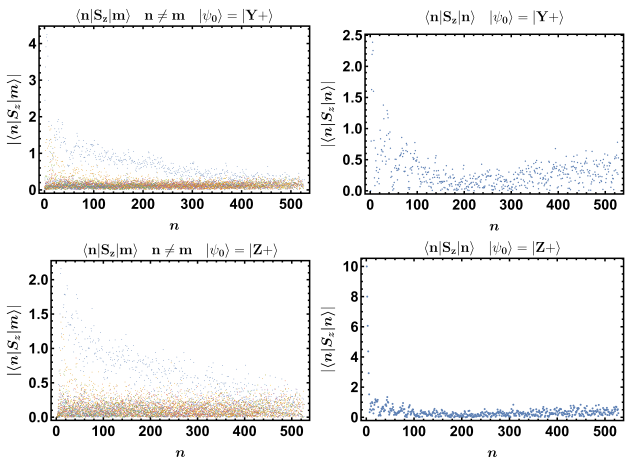

Fig. 5 Actual (absolute) values of matrix elements of the operator $S_z = \sum_i \sigma_i^z$ in Krylov basis for cases where the initial state is $|Y+\rangle$ (up) and $|Z+\rangle$ (down). Blue points in the left panels denote $(S_z)_{n,n+1}$ elements

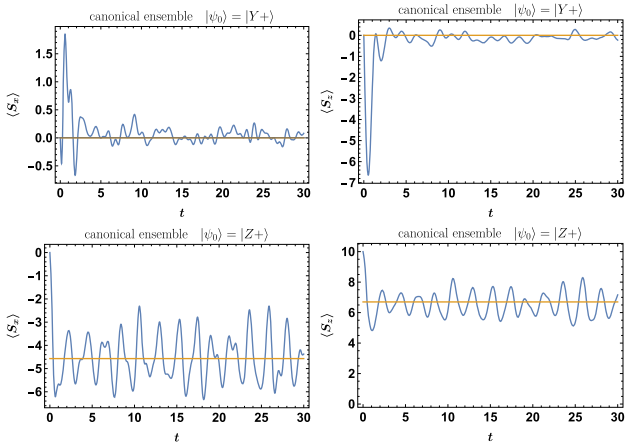

Fig. 6 Time evolution of the expectation value of S_x and S_z for two different initial states $|Y+\rangle$ (up) and $|Z+\rangle$ (down). The straight lines represent the value predicted by the canonical ensemble

for the Ising model (1) with $h = 0.5,\ g = -1.05$ where the model is non-integrable.

The corresponding matrix elements for two different initial states $|Y+\rangle$ and $|Z+\rangle$ are presented in Fig. 3 for $N = 10$. From this figure, one observes that the matrix elements O_{nm} exhibit the desired behavior as suggested by KTH. To highlight the behavior of matrix elements we have presented the absolute value of them, so that in Fig. 3 the dark points correspond to vanishing elements.

To further explore KTH we have also presented the actual values of matrix elements of S_x in the Krylov basis for different initial states in Fig. 4 where one can observe that $(S_x)_{n,n+1}$ is significantly greater than other elements. Note also that, diagonal elements $\mathcal{O}_{nn}$ are not entirely given by $f(a_0)$ and, in fact, they appear in a certain combination of $f(a_0) + (a_n - a_0) f'(a_0)$ which might be small, even though the expectation value, itself, could be relatively large.

We have also computed matrix elements of the magnetization in the z direction, $S_z = \sum_{i=1}^{N} \sigma_i^z$, for several initial states specified by different θ and ϕ and we have found the same pattern as that in Figs. 3 and 4. In particular, numerical results for initial states $|Y+\rangle$ and $|Z+\rangle$ are depicted in Fig. 5.

It is also illustrative to explicitly compute time evolution of the operator we considered above to see how they actually follow the general behavior given by the Eq. (39). The results are depicted in Fig. 6. The straight brown lines in these plots represent the long time expectation value predicted by the canonical ensemble which is equal to the infinite time average of the corresponding expectation value: $\mathrm{Tr}(\rho_{DE} S_{x,z}) \approx \mathrm{Tr}(\rho_{th} S_{x,z})$, that is necessary for thermalization to occur.

Although thermalization occurs for both initial states, from this figure one observes that the nature of thermalization should be different for these states. While $|Y+\rangle$ exhibit string thermalization, for $|Z+\rangle$ it is weak.

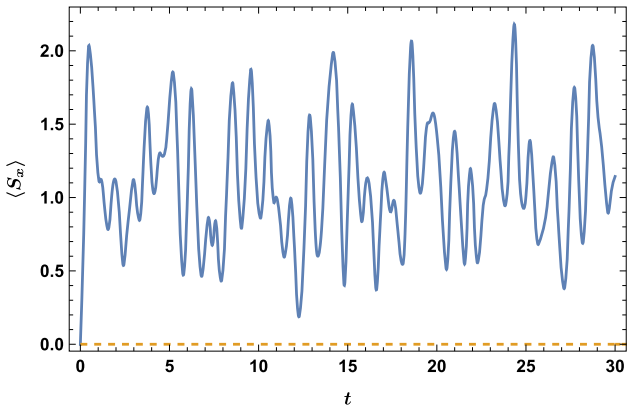

Fig. 7 Time evolution of the expectation value of S_x for initial state $|Y+\rangle$ for an integrable case where $h = 0$. The brown dashed line represents a value predicted by the canonical ensemble whose energy is the same as that of the initial state $|Y+\rangle$

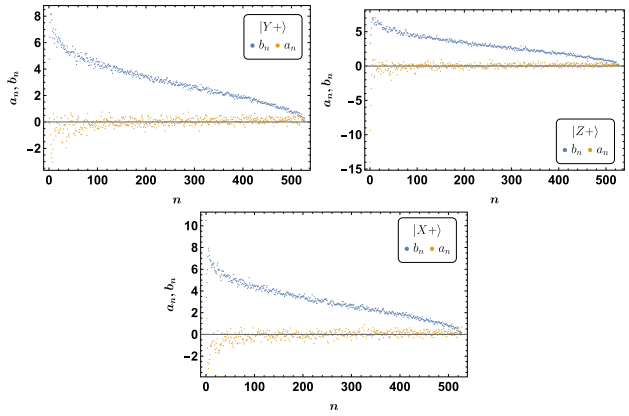

Fig. 8 Lanczos coefficients a_n, b_n of three initial states $|Y+\rangle, |Z+\rangle, |X+\rangle$. b_n and a_n are shown with blue and brown circles, respectively. The numerical results are presented for $N = 10$ in which the dimension of Krylov space for a generic initial state is about 528

To further explore the KTH behavior we have also done the same computations for the cases where $gh = 0$ in which the model (1) is integrable. An immediate observation we have made is that in integrable cases the dimension of Krylov space reduces significantly[8] which may also depend on the initial state. For example, for $N = 10$, where the dimension of the full Hilbert space is 2^{10}, in the chaotic case, the dimension of the Krylov space is 529.[9] In the integrable case with parameters $h = 0$ and $g = -1.05$, the corresponding dimensions are 463 for the initial states $|Y+\rangle$ and $|Z+\rangle$, and 253 for $|X+\rangle$.

In order to have a better statistic we have considered the case where $h = 0,\ g = -1.05$. For this case, we have computed matrix elements of different operators in the Krylov basis for different initial states. We have found that, although for some special cases, the corresponding matrix elements have almost similar patterns as that in Fig. 3, it is not a generic behavior and typically they exhibit non-universal behavior. More importantly, in this case the long time average cannot be approximated by a canonical ensemble (see, for example, Fig. 7).

3 Krylov space and nature of thermalization

As we have already maintained although both initial states $|Y+\rangle$ and $|Z+\rangle$ exhibit almost the same pattern for the operator matrix elements (see Figs. 4, 5) indicating that thermalization occurs in both states, it is evident for Fig. 6 that the nature of thermalization for these two states must be different, as we discussed in the previous section. In this section, we would like to study how the nature of thermalization, being weak or strong, can be probed in the context of Krylov space.

From Eq. (39) one finds that the nature of thermalization should be controlled by the second term which is essentially given by a summation over $\phi_n(t)$'s. On the other hand, $\phi_n(t)$ can be evaluated, recursively, from $\phi_0(t)$ using Lanczos coefficients. Therefore, the nature of thermalization should be reflected in these quantities. Based on this insight, we will propose various quantities within the framework of Krylov space that could serve as indicators for the nature of thermalization.

3.1 Variance of Lanczos coefficients

From the Krylov basis construction, it is evident that the Lanczos coefficients should encapsulate information about both the model's dynamics and initial state, making them a suitable candidate for probing the nature of thermalization.

To explore this idea, let us begin by calculating the Lanczos coefficients for three different initial states that we have discussed in the previous section.[10] The results for $N = 10$ are shown in Fig. 8

[8] Similar observation has been already made in the context of operator Krylov complexity in [19] (see also [20]).

[9] It is known that the Hamiltonian (1) has a parity symmetry which is essentially reflection symmetry about the center of the chain. It is straightforward to see that the initial state (6) has positive parity which in turn indicates that the obtained Krylov subspace should be a subspace with positive parity. Actually, the positive parity subspace has 528 dimensions, as expected, which is equal to the dimension of Krylov space.

[10] Lanczos coefficients for the model under consideration have also been computed in [21,24**? ?** –26].

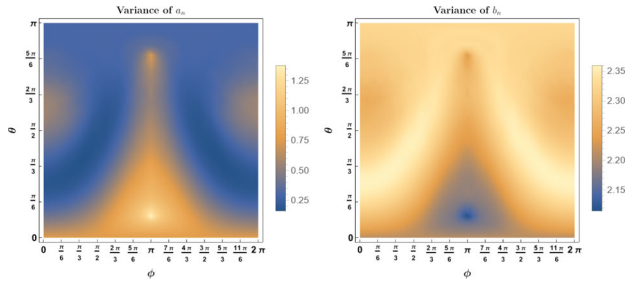

Fig. 9 Variance of Lanczos coefficients a_n (left) and b_n (right). The numerical results are done for $N = 10$ spins

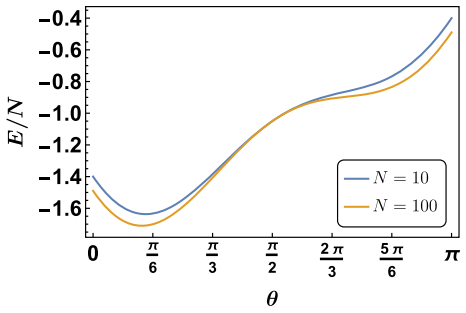

Fig. 10 Density of energy (left) and its derivative (right) for $\phi = \pi$ slice for different $N = 10, 100$. Indeed, they show nontrivial behavior around $\theta = \frac{5\pi}{6}$, though it is not as pronounced as that in the variance of a_n

Although one could recognize some differences among these three plots, the differences are not substantial. Essentially, the Lanczos coefficients exhibit qualitatively similar patterns across all three cases. As a result, one might conclude that the straightforward behavior of Lanczos coefficients may not offer a distinct metric to differentiate between these three cases.

We note, however, that a better quantity which might be more sensitive to the initial state is the variance of Lanczos coefficients. Indeed, the variance of Lanczos coefficients has been considered in [26] as a measure to probe whether a system is chaotic or integrable.

Let us recall that for a collection of M numbers, s_i, the variance may be defined as follows

$$\mathrm{Var}(s_i) = \frac{1}{M}\sum_{i=1}^{M}(s_i - \bar{s})^2 \tag{40}$$

where $\bar{s}$ is the mean value. In what follows we would like to compute the variance of Lanczos coefficients a_n and b_n. Actually, if one computes the variance of Lanczos coefficients for three initial states considered before, one observes that they differ significantly.

More generally, one could compute the variance of Lanczos coefficients associated with the general initial state given by (6). In Fig. 9 we have presented the numerical results for the variance of a_n and b_n as a function of θ and ϕ for $N = 10$.

Clearly, there is an obvious correlation between behaviors of the effective inverse temperature, the absolute value of the density of energy (or normalized energy) and variance of Lanczos coefficients (see Fig. 1). Generally, one observes that for regions where the effective inverse temperature is small the variance of a_n (b_n) is also small (large). The variance of a_n (b_n) becomes larger (smaller) as we move away from $\beta = 0$ regions. Another observation we have made is that being positive, the variance is not sensitive to the sign of β and only the absolute value of it matters.

We note, however, that the behavior of variances is not exactly the same as that of effective inverse temperature. Indeed, even though one can recognize the lower part of the ring of zero β, the upper part is not apparent in the plots of variances, though there is a trace of the ring. More precisely, although from the behavior of β or density of energy one would expect to see states with strong thermalization are localized near the ring of zero β, the behavior of the variance suggests that strong thermalization for states with $\theta \gtrsim \frac{2\pi}{3}$ does not necessarily located near the ring of zero β and rather they almost uniformly distribute around $\theta \approx \pi$.

Notably, along the symmetric axis at $\phi = \pi$, while the effective inverse temperature and the absolute value of the energy density decrease almost monotonically from $\theta = \frac{\pi}{6}$ to $\theta = \pi$, the variance of a_n exhibits a minimum around $\theta \approx \frac{5\pi}{6}$. This suggests that the state $|\frac{5\pi}{6}, \pi\rangle$ is among those with the weakest thermalization.

To validate our numerical results, we can leverage the exact analytic expression for the energy. This allows us to compute the energy density for the $\phi = \pi$ slice for arbitrary N. In Fig. 10, we present the energy density for $N = 10$ and $N = 100$ to further examine its behavior.

From this figure, we observe that the energy density exhibits non-trivial behavior around $\theta = \frac{5\pi}{6}$, though this is less pronounced than the variance of a_n. Using the explicit form of the energy density for large N given in Eq. (9), we can compute its derivative with respect to θ for the $\phi = \pi$ slice

$$E' = \frac{N}{2}\left(\sin\theta + 4\cos\theta\sin\theta - \frac{21}{10}\cos\theta\right), \tag{41}$$

where the prime indicates differentiation with respect to θ. The potential minima can be identified by solving the equation

$$\sin\theta + 4\cos\theta\sin\theta - \frac{21}{10}\cos\theta = 0\,. \tag{42}$$

It is straightforward to see that this equation has only one solution for $\theta \in [0, \pi]$. Therefore, while the second point may appear significant, there is no true minimum around $\theta =$

$\frac{5\pi}{6}$. Remarkably, for large N, the position of the minimum remains independent of N.

In conclusion, we find a correlation between the behavior of the effective inverse temperature and the variance of the Lanczos coefficients. However, notable discrepancies persist between the two, suggesting that the variance of the Lanczos coefficients may not be a reliable indicator of the nature of thermalization, despite its potential to capture certain aspects of it.

3.2 Infinite time average of Krylov complexity

Working with Krylov basis we note that there is rather a special operator in Krylov space whose matrix elements are proportional to Kronecker delta. More precisely, consider the number operator defined by

$$\mathcal{N} = \sum_{n=0}^{\mathcal{D}_\psi - 1} n|n\rangle\langle n|, \tag{43}$$

that is obviously diagonal in Krylov basis, $\mathcal{N}_{nm} = n\delta_{nm}$. We note that the expectation value of the number operator, actually, computes Krylov complexity [8][11]

$$\mathcal{C} = \langle \mathcal{N}(t)\rangle = \sum_{n=0}^{\mathcal{D}_\psi - 1} n\ |\phi_n(t)|^2\,, \tag{44}$$

that saturates at very late times where the Lanczos coefficients vanish [34]. The Krylov complexity is an interesting quantity which relies on both the initial state and the Hamiltonian, akin to Lanczos coefficients.

The evolution of maximally entangled states in the Krylov basis has been studied in [35], revealing that the growth and subsequent saturation of Krylov complexity are common features of many-body systems, regardless of their chaotic or integrable nature. As a general consequence, we would expect to observe the following behavior at late times

$$\mathcal{C} = \overline{\mathcal{C}} + \text{small fluctuations}\,, \tag{45}$$

where $\overline{\mathcal{C}}$ is the infinite time average of the Krylov complexity given by

$$\overline{\mathcal{C}} = \lim_{T\to\infty} \frac{1}{T}\int_0^T \langle \mathcal{N}(t)\rangle\, dt = \mathrm{Tr}(\rho_{DE}\mathcal{N})\,, \tag{46}$$

It was conjectured that one could probe the system's dynamics by examining the infinite time average of Krylov complexity, with chaotic models exhibiting higher values

[11] See also [27–33] for related works.

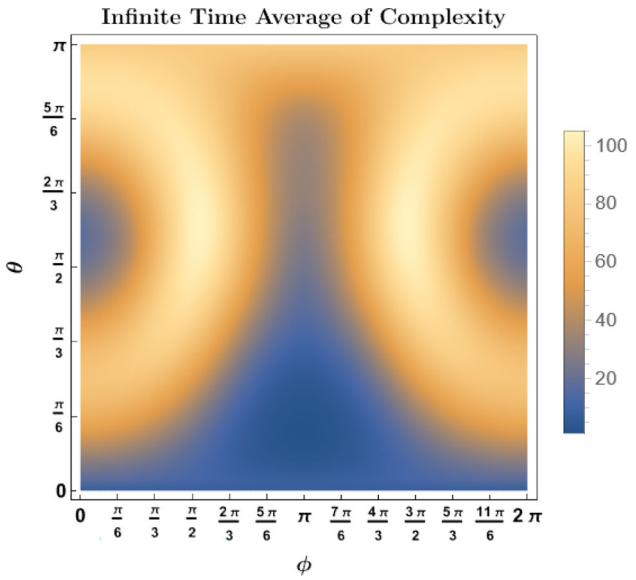

Fig. 11 Infinite time average of complexity for states associated with the initial state 6. The numerical computation is done for $N = 9$

[36]. In fact, in an explicit Ising model, it has been demonstrated in [36] that the infinite time average of the Krylov complexity increases as one transitions from an integrable model to a chaotic one. However, it is important to note that in addition to the dynamics the infinite time average of Krylov complexity also depends on the initial states. In fact, the infinite time average of Krylov complexity for chaotic systems may or may not exceed that of integrable models [22,23,26].

We have leveraged this insight to propose the infinite time average of Krylov complexity as a measure to probe the nature of thermalization. It is straightforward to compute the infinite time average of complexity for states associated with initial states (6). The numerical result for $N = 9$ is depicted in Fig. 11.

Interestingly, the resulting pattern aligns perfectly with the absolute value of the energy density and the effective inverse temperature. Specifically, we have observed that states exhibiting strong thermalization have a higher complexity saturation value than those with weak thermalization. In conclusion, for the model described in Eq. (1), we find that as thermalization intensifies, the complexity saturation value also increases. We hypothesize that similar conclusions may apply to generic models.

3.3 Inverse participation ratio

It is worth mentioning that by making use of the inverse participation ratio [37] the nature of weak or strong thermalization of certain XY Ising model has been studied in [38]. Thus it is worth looking at this quantity for our model too.

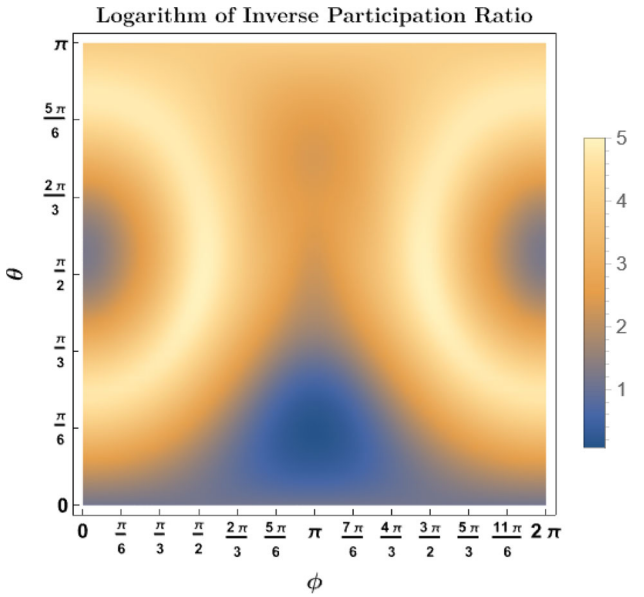

Fig. 12 The logarithm of inverse participation ratio for general initial state given in (6) as a function of θ and ϕ. The numerical computation is done for $N = 10$

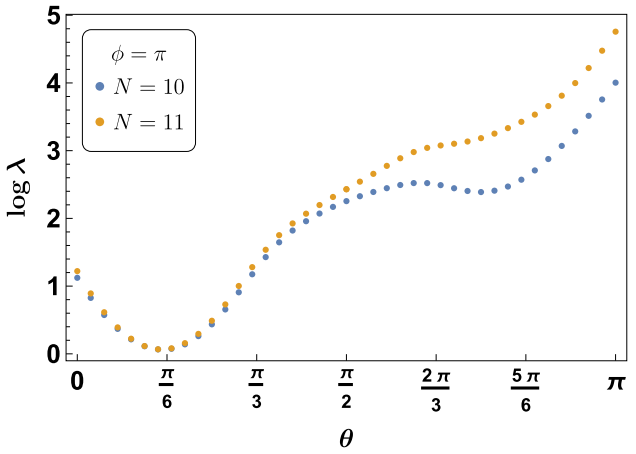

Fig. 13 The logarithm of inverse participation ratio of $\phi = \pi$ slice for $N = 10, 11$. One observes that the second peak (minimum) is removed as one goes to higher N

Consider a state whose expansion in the energy eigenstates is $|\psi\rangle = \sum_{\alpha=1}^{\mathcal{D}} c_\alpha |E_\alpha\rangle$, where $c_\alpha = \langle E_\alpha|\psi\rangle$. Then, the inverse participation ratio is defined by

$$\lambda = \frac{1}{\sum_{\alpha=1}^{\mathcal{D}} |c_\alpha|^4} = \frac{1}{\mathrm{Tr}(\rho_{DE}^2)}\,, \tag{47}$$

which is essentially a quantity that measures the number of energy eigenstates that contribute to the state $|\psi\rangle$. Note that $1 \leq \lambda \leq \mathcal{D}$. In fact, when only one energy eigenstate contributes to the state the inverse participation number is one, while when all energy levels equally contribute to the state it is equal to $\mathcal{D}$.

It is worth also noting that the inverse participation ratio may be given in terms of the infinite time average of the wave function ϕ_0

$$\lambda^{-1} = \lim_{T\to\infty} \frac{1}{T} \int_0^T |\phi_0(t)|^2 dt\,. \tag{48}$$

Now, let us compute the inverse participation ratio for the general initial state (6). The results are depicted in Fig. 12, which displays the logarithm of the inverse participation ratio, $\ln \lambda$. Interestingly enough, there is a strong correlation with all the quantities we have examined thus far, including the variance of the Lanczos coefficients.

It is important to highlight that analyses of the effective inverse temperature and normalized energy suggest weak thermalization occurs for states near the edge of the energy spectrum [3–6]. In our investigation, we found a correlation between whether a state exhibits weak or strong thermalization and its inverse participation ratio, as indicated in [38]. Specifically, the nature of a state's thermalization is closely linked to the number of energy eigenstates contributing to it; states comprised of more energy eigenstates tend to display stronger thermalization. Our computations of the expectation values of local operators further confirm this behavior.

Moreover, the behavior of the (log) inverse participation ratio aligns perfectly with the infinite time average of complexity. This indicates that the saturation value of complexity is higher for states composed of a greater number of energy eigenstates [26,36].

It is intriguing to observe that when examining the $\phi = \pi$ slice, we see a behavior similar to the variance of the Lanczos coefficients. Specifically, there are two distinct minima located around $\frac{\pi}{6}$ and $\frac{5\pi}{6}$. However, it is important to note that the first minimum corresponds to the state with the weakest thermalization, while the second minimum is an artifact of the finite N effect. To illustrate this, we present the logarithm of the inverse participation ratio for $N = 10$ and $N = 11$ in Fig. 13, which clearly shows that the second minimum disappears as we increase N. Interestingly, the corrections associated with larger N do not significantly alter the other characteristics of the inverse participation ratio.

To conclude we note that for $N = 11$, the behavior of the inverse participation ratio at $\phi = \pi$ closely resembles that of the energy density, with only one true minimum present; the second minimum is not genuine (see Fig. 10).

3.4 Time dependent of expectation value

So far, we have investigated several measures to probe the nature of thermalization. It is important to note that our understanding of which states exhibit strong or weak thermalization is derived from energy behavior, or equivalently, from

the infinite time average of complexity and the inverse participation ratio, as shown in the Figs. 1, 11 and 12, respectively.

From these figures, we observe that the state associated with $\theta = 0$ (arbitrary ϕ), corresponding to $|Z+\rangle$, exhibits weak thermalization. In contrast, the state at $\theta = \pi$ (arbitrary ϕ), corresponding to $|Z-\rangle$, demonstrates strong thermalization. As θ transitions from 0 to π, a non-trivial behavior emerges, which is evident in the aforementioned figures.

To validate this expectation, we can compute the expectation value of a typical operator across different states to determine if they exhibit strong or weak thermalization. In fact, to get a better understanding of what actually happens in different points in the $\theta - \phi$ plane (initial states), we will consider the magnetization in the z direction and compute the following quantity[12]

$$\langle S_z(t)\rangle = \langle \theta, \phi | e^{-iHt} \sum_{i=1}^{N} \sigma_i^z e^{iHt} | \theta, \phi \rangle \,, \tag{49}$$

for different values of θ and ϕ. In examining the behavior of this expectation value, we note distinct characteristics for strong and weak thermalization. In the strong case, we observe a swift relaxation characterized by a quick rise or fall of the expectation value, followed by a saturation phase around the thermal value, with minor fluctuations. Conversely, weak thermalization shows oscillatory behavior from the outset, oscillating around the thermal value.

To quantify these behaviors, we calculate the ratio of the oscillation size (variance of the oscillation) to the amplitude of the first peak or trough following relaxation. This ratio serves as an indicator of thermalization strength: for states exhibiting weak thermalization, the ratio approaches one, whereas for states with strong thermalization, it is significantly less than one. By assessing this ratio for a specific initial state, we can determine its tendency toward either strong or weak thermalization. For instance, for the state $|y+\rangle$, which is expected to exhibit strong thermalization, the ratio is about 0.01, while for the states $|Z+\rangle$ and $|Z+\rangle$, it is about 0.5 and 0.7, respectively.

By exploring various initial states, we have found perfect agreement with our expectations based on the behavior of energy. Actually, we have computed the corresponding expectation value for 441 initial states[13] and only few of them have been shown in this Fig. 14 which are for particular slices given by $\phi = 0, \pi$. The results are relatively compatible with what suggested by the variance of Lanczos coefficients and in exact agreement with what is suggested by the infinite time average of complexity.

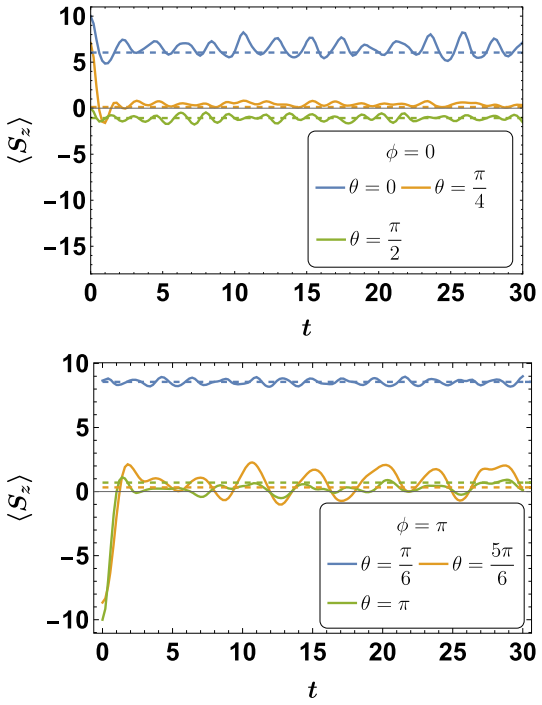

Fig. 14 Expectation value of S_z as a function of time for different initial states. As we see the weakest thermalization mostly occurs for states whose theta angle is near zero while beside the ring of zero β the strong thermalization occurs for $\theta \approx \pi$

To further explore this point let us look at $\phi = 0$ slice where we have presented results for different values of θ in Fig. 14. By making use of these results we find weak thermalization at $\theta = 0$, strong thermalization around $\theta = \pi/4$, weak thermalization again at $\theta = \pi/2$, and finally strong thermalization as we approach $\theta = \pi$. Interestingly enough, we have found that the behavior is consistent with the behavior of the infinite time average of complexity.

Looking at $\phi = \pi$ slice, from the expectation value of S_z we find that the weakest thermalization occurs at $\theta \approx \frac{\pi}{6}$ while it becomes relatively stronger as we move towards $\theta = \pi$. Actually evaluating the energy expectation value, one can see that the initial state $|\frac{\pi}{6}, \pi\rangle$ is very close to an eigenstate of the Hamiltonian. Thus being localized in energy eigenstates one observes an oscillatory behavior for typical operators. This can also be seen from the inverse participation number in which for this state one has $\lambda \approx 1$.

It is worth also noting that we did not observe any further special point in this slice in agreement with the behavior of the infinite time average of complexity and in contrast to the behavior suggested by the variance in which we would expect to have a state with relatively weaker thermalization around $\theta \approx \frac{5\pi}{6}$.

[12] We have also computed the expectation value for the magnetization in the x direction, S_x, in which we have found that the conclusion is the same as that of S_z that is explicitly presented in what follows.

[13] Since the pattern in the Fig. 9 is symmetric under $\phi \to 2\pi - \phi$, we have only considered initial states located in $0 \le \phi \le \pi$.

4 Discussions

In this paper, we have studied thermalization for a closed quantum system using the Krylov basis. Actually, our main motivation to do so is that, by definition, under time evolution a quantum state propagates over a subspace of Hilbert space known as Krylov space. An advantage (at least theoretically) of working in this space is that we will have to deal with a space whose dimension is usually smaller than the dimension of the full Hilbert space.

In the traditional approach to quantum thermalization one usually has to study the expectation value of operators in the energy eigenstates. It is believed that for a chaotic quantum system the thermalization occurs in the level of eigenstates that mathematically reflected in the statement of ETH.

On the other hand, working within the context of Krylov space, one will have to compute matrix elements of local operators in the Krylov basis. It is then natural to expect that a similar concept may also show up in this context. Indeed, by making use of an explicit example we have shown that the matrix elements of local operators satisfy a condition analogous to that of ETH. More precisely, We have demonstrated that for thermalization to occur, the matrix representation of typical local operators in the Krylov basis should exhibit a specific tridiagonal form with all other elements in the matrix being exponentially small.

We have also studied the nature of thermalization in this framework by introducing certain metrics to probe whether a given initial state exhibits weak or strong thermalization. To do so, We have observed that the nature of thermalization depends on two crucial factors: the system's Hamiltonian and the initial state. The Krylov basis and Lanczos coefficients, by construction, contain information about these elements, making them capable for studying the process of thermalization.

We have shown that the infinite time average of Krylov complexity could provide a measure to probe the nature of thermalization[14] which is in perfect agreement with the behavior of the effective inverse temperature and the density of energy. In particular, an initial state exhibiting strong thermalization has relatively larger value for complexity saturation.

We have also suggested that the variance of Lanczos coefficients could probe the nature of thermalization to see whether for a given initial state the thermalization is weak or strong, too. We have seen that a state with relatively smaller (greater) variance for Lanczos coefficients a_n (b_n) exhibits strong (weak) thermalization. Of course, there is some mismatch between the variance of Lanczos coefficients and the other quantities we have evaluated. We believe that this miss match might be due to the finite N effect, though to explicitly show it we need to go to sufficiently higher N and perform our numerical computations with extremely high precision which is out of our computational abilities. We leave exploring this point for further study.

To further explore the thermalization properties of the model under consideration we have also evaluated the inverse participation ratio for general initial states. We have observed that strong thermalization occurs for states with relatively greater inverse participation ratio. In other words, a state consisting of more energy eigenstates is more likely to exhibit stronger thermalization. We have seen that there is a correlation between the behaviors of the infinite time average of complexity and the inverse participation ratio.

To verify our proposal we have also computed time dependence of the expectation value of local operators to explicitly probe the nature of thermalization for the generic initial state given by (6). The results, indeed, confirm our observation based on the behaviors of the infinite time average complexity, the inverse participation ratio and the variance of Lanczos coefficients.

An interesting question we have been trying to address rather implicitly in this paper was the robustness of the quantities we have studied in this paper against the size of the system. In most numerical computations we have done in this paper we have set $N = 10$, while in the literature the computations are done for $N = 14$. It is then natural to see how robust the results are.

Actually, among all the quantities we have considered in this paper, we have presented an exact analytic expression for expectation value of energy which may be treated as a gauge to validate other results.

It is clear from the exact analytic expression that for large N limit the density of energy is independent of N, so that its behavior is universal which only depends on the parameters of the model g and h.

We have also computed effective inverse temperature for $N = 7$ and, surprisingly, one observes that it perfectly agrees with the density of energy even for large N, showing that the behavior of β is robust against the size of the system. Of course, as we have already mentioned the actual value of β is changed, though in comparison with the numerical results available in the litterateur for $N = 14$ one finds just a few percent errors. It is worth emphasizing that this is also the case for other quantities we have studied in this paper that include the infinite time average of complexity, the inverse participation number and the expectation value of local operators. We note, however, that for the variance of Lanczos coefficients, we expect to see significant finite N effect to make it consistent with other quantities.

To explore our idea about thermalization in the Krylov basis we have considered an Ising model whose Hamiltonian is given by (1). We note, however, that there is another model

[14] We also note that a certain state dependence of Krylov complexity has been studied in [39].

which has been extensively studied in the literature whose Hamiltonian is

$$H = \sum_{i=1}^{N-1} \sigma_i^x \sigma_{i+1}^x + \sigma_i^y \sigma_{i+1}^y + g \sum_{i=1}^{N} \sigma_i^y \,. \tag{50}$$

For the general initial state (6) the expectation value of the energy is

$$E = \sin\theta \left((N-1)\sin\theta + Ng \sin\phi\right) \,. \tag{51}$$

One may also explore thermalization and its nature for this model by evaluating different quantities such as effective inverse temperature and infinite time average of complexity. Doing so, one can see that the results are consistent with the behavior of the expectation of the energy (51), that also confirms our expectations. We note that the inverse participation ratio for this model has been studied in [38].

In this paper, we have studied the infinite time average of the Krylov complexity and the variance of Lanczos coefficients associated with the spread of an initial state [40]. We note, however, that the same question as studied in this paper can be also addressed using Lanczos coefficients associated with operator growth [8].[15] Essentially in our context, it corresponds to changing the picture from Schrödinger to Heisenberg.

In the Heisenberg picture of quantum mechanics, we are dealing with the operators and the time evolution is attributed to the operator

$$\mathcal{O}(t) = e^{-iHt} \mathcal{O} e^{iHt} \,. \tag{52}$$

Defining an inner product in the space of operators acting on the Hilbert space, one can construct the Krylov basis for the operator starting with an initial operator $\mathcal{O}$. The first element is identified with the initial operator $O_0 = \mathcal{O}$ (which we assume to be normalized with respect to the inner product) and the other elements may be constructed recursively as follows

$$\hat{O}_{n+1} = \mathcal{L} O_n - \hat{b}_n O_{n-1}, \quad O_n = \hat{b}_n^{-1} \hat{O}_n, \tag{53}$$

where $\mathcal{L} O_n = [H, O_n]$ and $\hat{b}_n^2 = |\hat{O}_n \cdot \hat{O}_n|$ is Lanczos coefficients. The procedure stops for $n = \mathcal{D}_O \leq \mathcal{D}^2 - \mathcal{D} + 1$ [19] that is the dimension of Krylov space for the operator. Here we denote the Lanczos coefficients with a hat to avoid confusion with those defined in the Krylov basis for state in (15). Using this basis one has

$$\mathcal{O} = \sum_{n=1}^{\mathcal{D}_O - 1} i^n \, \varphi_n(t) \, O_n \,. \tag{54}$$

Note that with this notation $\varphi_n(t)$ is real and satisfies the following equation

$$\partial_t \varphi_n(t) = \hat{b}_n \varphi_{n-1} - \hat{b}_{n+1} \varphi_{n+1} \,. \tag{55}$$

In this context, we could also look for the variance of Lanczos coefficients in the operator picture. To study Lanczos coefficients for the Ising model (1) we may consider a generic initial operator as follows

$$\mathcal{O}_{\theta,\phi} = \prod_{i=1}^{N} \mathcal{O}_i(\theta, \phi), \tag{56}$$

where $\mathcal{O}_i$ is defined in (7). It is worth noting that since this initial state (6) is the eigenstate of the above operator, in this case, we are essentially studying the time evolution of density matrix associated with the initial state $\mathcal{O}_{\theta,\phi} = \rho(\theta, \phi) = |\theta, \phi\rangle\langle\theta, \phi|$.

One can also study the variance of Lanczos coefficients $\hat{b}_n$ associated with the initial density matrix. Doing so, one finds the corresponding variance results in the same conclusion as that for the state studied in the previous section. An interesting observation we have made is that the behavior of variance $\hat{b}_n$ in operator growth is actually identical with that obtained from a_n in state growth. It would be interesting to understand this point better.

Acknowledgements We would like to thank Ali Mollabashi, Mohammad Reza Mohammadi Mozaffar, Mohammad Reza Tanhayi and Hamed Zolfi for useful discussions. We would also like to thank the School of Physics of the Institute for Research in Fundamental Sciences (IPM) for providing computational facilities. M.A. would also like to thank Souvik Banerjee for discussions on different aspects of Krylov space. Some numerical computations related to this work were carried out at IPM Turin Cloud Services [42]. This work is based upon research founded by Iran National Science Foundation (INSF) under project No 4023620.

Data Availability Statement This manuscript has no associated data. [Authors' comment: This study did not generate any data that can be shared publicly.]

Code Availability Statement The manuscript has no associated code/software. [Author's comment: Code/Software sharing not applicable to this article as no code/software was generated or analysed during the current study.]

[15] We note that operator and state growth may be studied within a universal framework [41].

Funded by SCOAP[3].

References

1. M. Srednicki, Chaos and quantum thermalization. Phys. Rev. E **50**, 888. https://doi.org/10.1103/PhysRevE.50.888. arXiv:cond-mat/9403051
2. J.M. Deutsch, Quantum statistical mechanics in a closed system. Phys Rev A. **43**, 2046 (1991). https://doi.org/10.1103/physreva.43.2046
3. M.C. Bañuls, J.I. Cirac, M.B. Hastings, Strong and weak thermalization of infinite nonintegrable quantum systems. Phys. Rev. Lett. **106**(5), 050405 (2011). https://doi.org/10.1103/PhysRevLett.106.050405
4. Z.H. Sun, J. Cui, H. Fan, Quantum information scrambling in the presence of weak and strong thermalization. Phys. Rev. A **104**(2), 022405 (2021). https://doi.org/10.1103/PhysRevA.104.022405. arXiv:2008.01477 [quant-ph]
5. F. Chen et al., Observation of strong and weak thermalization in a superconducting quantum processor. Phys. Rev. Lett. **127**, 020602 (2021). https://doi.org/10.1103/PhysRevLett.127.020602
6. C.J. Lin, O.I. Motrunich, Quasiparticle explanation of the weak-thermalization regime under quench in a nonintegrable quantum spin chain. Phys. Rev. A **95**(2), 023621 (2017). https://doi.org/10.1103/PhysRevA.95.023621. arXiv:1610.04287 [cond-mat.stat-mech]
7. V.S. Viswanath, G. Mülle, *The Recursion Method: Application to Many Body Dynamics* Lecture Notes in Physics Monographs. (Springer, Berlin, 1994)
8. D.E. Parker, X. Cao, A. Avdoshkin, T. Scaffidi, E. Altman, A universal operator growth hypothesis. Phys. Rev. X **9**(4), 041017 (2019). https://doi.org/10.1103/PhysRevX.9.041017. arXiv:1812.08657 [cond-mat.stat-mech]
9. O. Bohigas, M.J. Giannoni, C. Schmit, Characterization of chaotic quantum spectra and universality of level fluctuation laws. Phys. Rev. Lett. **52**, 1–4 (1984). https://doi.org/10.1103/PhysRevLett.52.1
10. M. Srednicki, The approach to thermal equilibrium in quantized chaotic systems. J. Phys. A Math. Gen. **1163** (1999)
11. I. Dumitriu, A. Edelman, Matrix models for beta ensembles. arXiv:math-ph/0206043
12. V. Balasubramanian, J.M. Magan, Q. Wu, Tridiagonalizing random matrices. Phys. Rev. D **107**(12), 126001 (2023). https://doi.org/10.1103/PhysRevD.107.126001. arXiv:2208.08452 [hep-th]
13. V. Balasubramanian, J.M. Magan, Q. Wu, Quantum chaos, integrability, and late times in the Krylov basis. arXiv:2312.03848 [hep-th]
14. J.L.F. Barbón, E. Rabinovici, R. Shir, R. Sinha, On the evolution of operator complexity beyond scrambling. JHEP **10**, 264 (2019). https://doi.org/10.1007/JHEP10(2019)264. arXiv:1907.05393 [hep-th]
15. B. Bhattacharjee, S. Sur, P. Nandy, Probing quantum scars and weak ergodicity breaking through quantum complexity. Phys. Rev. B **106**(20), 205150 (2022). https://doi.org/10.1103/PhysRevB.106.205150. arXiv:2208.05503 [quant-ph]
16. C. Lanczos, An iteration method for the solution of the eigenvalue problem of linear differential and integral operators. J. Res. Natl. Bur. Stand. B **45**, 255–282 (1950). https://doi.org/10.6028/jres.045.026
17. L. D'Alessio, Y. Kafri, A. Polkovnikov, M. Rigol, From quantum chaos and eigenstate thermalization to statistical mechanics and thermodynamics. Adv. Phys. **65**(3), 239–362 (2016). https://doi.org/10.1080/00018732.2016.1198134. arXiv:1509.06411 [cond-mat.stat-mech]
18. T. Mori, T.N. Ikeda, E. Kaminishi, M. Ueda, Thermalization and prethermalization in isolated quantum systems: a theoretical overview. J. Phys. B **51**(11), 112001 (2018). https://doi.org/10.1088/1361-6455/aabcdf. arXiv:1712.08790 [cond-mat.stat-mech]
19. E. Rabinovici, A. Sánchez-Garrido, R. Shir, J. Sonner, Operator complexity: a journey to the edge of Krylov space. JHEP **06**, 062 (2021). https://doi.org/10.1007/JHEP06(2021)062. arXiv:2009.01862 [hep-th]
20. P. Caputa, H.S. Jeong, S. Liu, J.F. Pedraza, L.C. Qu, Krylov complexity of density matrix operators. arXiv:2402.09522 [hep-th]
21. J.D. Noh, Operator growth in the transverse-field Ising spin chain with integrability-breaking longitudinal field. arXiv:2107.08287
22. B.L. Español, D.A. Wisniacki, Assessing the saturation of Krylov complexity as a measure of chaos. Phys. Rev. E **107**(2), 024217 (2023). https://doi.org/10.1103/PhysRevE.107.024217. arXiv:2212.06619 [quant-ph]
23. F.B. Trigueros, C.J. Lin, Krylov complexity of many-body localization: Operator localization in Krylov basis. SciPost Phys. **13**(2), 037 (2022). https://doi.org/10.21468/SciPostPhys.13.2.037. arXiv:2112.04722 [cond-mat.dis-nn]
24. A. Bhattacharya, P. Nandy, P.P. Nath, H. Sahu, On Krylov complexity in open systems: an approach via bi-Lanczos algorithm. JHEP **12**, 066 (2023). https://doi.org/10.1007/JHEP12(2023)066. arXiv:2303.04175 [quant-ph]
25. A. Bhattacharya, P. Nandy, P.P. Nath, H. Sahu, Operator growth and Krylov construction in dissipative open quantum systems. JHEP **12**, 081 (2022). https://doi.org/10.1007/JHEP12(2022)081. arXiv:2207.05347 [quant-ph]
26. G.F. Scialchi, A.J. Roncaglia, D.A. Wisniacki, Integrability to chaos transition through Krylov approach for state evolution. arXiv:2309.13427 [quant-ph]
27. A. Avdoshkin, A. Dymarsky, Euclidean operator growth and quantum chaos. Phys. Rev. Res. **2**(4), 043234 (2020). https://doi.org/10.1103/PhysRevResearch.2.043234. arXiv:1911.09672 [cond-mat.stat-mech]
28. A. Dymarsky, A. Gorsky, Quantum chaos as delocalization in Krylov space. Phys. Rev. B **102**(8), 085137 (2020). https://doi.org/10.1103/PhysRevB.102.085137. arXiv:1912.12227 [cond-mat.stat-mech]
29. A. Dymarsky, M. Smolkin, Krylov complexity in conformal field theory. Phys. Rev. D **104**(8), L081702 (2021). https://doi.org/10.1103/PhysRevD.104.L081702. arXiv:2104.09514 [hep-th]
30. J. Kim, J. Murugan, J. Olle, D. Rosa, Operator delocalization in quantum networks. Phys. Rev. A **105**(1), L010201 (2022). https://doi.org/10.1103/PhysRevA.105.L010201. arXiv:2109.05301 [quant-ph]
31. K. Adhikari, S. Choudhury, A. Roy, Krylov complexity in quantum field theory. Nucl. Phys. B **993**, 116263 (2023). https://doi.org/10.1016/j.nuclphysb.2023.116263. arXiv:2204.02250 [hep-th]
32. H.A. Camargo, V. Jahnke, H.S. Jeong, K.Y. Kim, M. Nishida, Spectral and Krylov complexity in billiard systems. Phys. Rev. D **109**(4), 046017 (2024). https://doi.org/10.1103/PhysRevD.109.046017. arXiv:2306.11632 [hep-th]
33. K.B. Huh, H.S. Jeong, J.F. Pedraza, Spread complexity in saddle-dominated scrambling. arXiv:2312.12593 [hep-th]
34. E. Rabinovici, A. Sánchez-Garrido, R. Shir, J. Sonner, Krylov complexity from integrability to chaos. JHEP **07**, 151 (2022). https://doi.org/10.1007/JHEP07(2022)151. arXiv:2207.07701 [hep-th]

35. J. Erdmenger, S.K. Jian, Z.Y. Xian, Universal chaotic dynamics from Krylov space. JHEP **08**, 176 (2023). https://doi.org/10.1007/JHEP08(2023)176. arXiv:2303.12151 [hep-th]
36. E. Rabinovici, A. Sánchez-Garrido, R. Shir, J. Sonner, Krylov localization and suppression of complexity. JHEP **03**, 211 (2022). https://doi.org/10.1007/JHEP03(2022)211. arXiv:2112.12128 [hep-th]
37. A.J. Short, T.C. Farrelly, Quantum equilibration in finite time. New J. Phys. **14**(1), 013063 (2012). https://doi.org/10.1088/1367-2630/14/1/013063. arXiv:1110.5759 [quant-ph]
38. L.F. Prazeres, T.R. de Oliveira, Continuous transition between weak and strong thermalization using rigorous bounds on equilibration of isolated systems. arXiv:2310.13392 [quant-ph]
39. A. Kundu, V. Malvimat, R. Sinha, State dependence of Krylov complexity in 2d CFTs. JHEP **09**, 011 (2023). https://doi.org/10.1007/JHEP09(2023)011. arXiv:2303.03426 [hep-th]
40. V. Balasubramanian, P. Caputa, J.M. Magan, Q. Wu, Quantum chaos and the complexity of spread of states. Phys. Rev. D **106**(4), 046007 (2022). https://doi.org/10.1103/PhysRevD.106.046007. arXiv:2202.06957 [hep-th]
41. M. Alishahiha, S. Banerjee, A universal approach to Krylov state and operator complexities. SciPost Phys. **15**(3), 080 (2023). https://doi.org/10.21468/SciPostPhys.15.3.080. arXiv:2212.10583 [hep-th]
42. https://turin.ipm.ir/